Design of a Fast Real-Time LPV Model Predictive Control System for Semi-Active Suspension Control of a Full Vehicle

Marcelo Menezes Morato, Manh Quan Nguyen, Olivier Sename, Luc Dugard

Design of a Fast *Real-Time LPV* Model Predictive Control System for Semi-Active Suspension Control of a Full Vehicle

Marcelo Menezes Morato[a,b], Manh Quan Nguyen[b], Olivier Sename[b], Luc Dugard[b]

[a] *Departamento de Automação e Sistemas (*DAS*), Universidade Federal de Santa Catarina, Florianópolis, Brazil*
[b] *Université Grenoble Alpes, CNRS, Grenoble INP$^{\top}$, GIPSA-lab, 38000 Grenoble, France*

Abstract

This article is concerned with the control of a Semi-Active suspension system of a 7DOF Full Vehicle model, equipped with four *Electro Rheological* (*ER*) dampers, taking into account their incipient dissipativity constraints. Herein, a Real-Time, fast, advanced control structure is presented within the Model Predictive Control framework for Linear Parameter Varying (LPV) systems. The control algorithm is developed to provide a suitable trade-off between comfort and handling performances of the vehicle in a very limited sampling period ($T_s = 5\,\text{ms}$), in the view of a possible realtime implementation on a real vehicle. The control structure is tested and compared to other standard fast control approaches. Full nonlinear realistic simulation results illustrate the overall good operation and behaviour of the proposed control approach.

Keywords: Fast Model Predictive Control, LPV Control, Vehicle Systems, Semi-Active Suspensions, Suboptimal Optimization, H_2 Extended Observer

Email addresses: marcelomnzm@gmail.com (Marcelo Menezes Morato), quannm.ii@gmail.com (Manh Quan Nguyen), olivier.sename@gipsa-lab.fr (Olivier Sename), L.Dugard@gipsa-lab.fr (Luc Dugard)

1. Introduction

In order to enhance a vehicle's driving performance in terms of road handling and ride comfort, one should take special care with the vehicle's suspension system. More and more present in the automotive industry, *Semi-Active* suspension systems should be highlighted, being efficient and, at the same time, less energy-consuming and less expensive than purely active suspensions.

1.1. Semi-Active Suspension Systems

The use of semi-active suspension systems provides a good trade-off between costs and performance requirements. This type of suspension is present on recent *state-of-the-art top*-cars and a good deal of academic and industrial research works have been focused on this topic, as seen in [1, 2, 3] and others. Further details on semi-active suspension systems are thoroughly discussed in [4, 5].

The main challenge faced by semi-active suspension control problems is how to handle the **dissipativity constraints** of these dampers. Several control design problems have been worked out with a range of different approaches. In [6] and [7], we can find an extensive review of approaches towards semi-active suspension control; the references therein can provide more details and serve for further studies for readers. Indeed, some of the most recent and modern control techniques have been applied for this problem. In [1], an LQ-based clipped optimal control is proposed; an H_∞ control approach is presented in [8]; LPV control approaches, dealing with the dissipativity constraints of these suspension systems, are given in [9, 10]; a robust control approach with input and state constraints is developed in [11].

1.2. Why Model Predictive Control?

Nevertheless, a more natural approach towards optimal control of processes subject to constraints is the Model Predictive Control (MPC) framework, as thoroughly introduced in [12]. MPC allows to explicitly consider the effect of input (actuator) and state constraints in the control design process. This

framework has been used as a solution to deal with many kinds of processes, such as energy plants [13], and various kinds of goals, even serving as fault-tolerant control schemes [14, 15].

The control of semi-active suspension systems consists in manipulating the damping coefficient of a controlled damper, the actuator from the system's point-of-view. Semi-active dampers have dissipativity constraints that can be tackled elegantly as an actuator saturation problem within the *MPC* framework.

Some works have employed an *MPC* approach for semi-active suspension systems, although most of these studies only consider a simpler *quarter-car* vehicle model. However, the *quarter-car* model (and *half-car* model as well) is not sufficient to describe the dynamics of a full vehicle with four semi-active dampers. The idea of solving the control problem at each corner of the car (four separate controllers) might seem appealing and simple enough, but the effects of coupling and load transfer distribution between corners may not be handled, which should lead to degraded performance, as discussed in [16]. Still on this matter, this solution presents its difficulties for a real-time implementation, given that four control laws have to computed within the sampling period.

The following references are emphasized:

Considering *quarter-car* models:

- In [17], a *fast MPC* scheme is designed for a *quarter-car* vehicle model, but the computation of the control law is sub-optimal, due to conditional constraints;
- In [18], a methodology is proposed for optimal semi-active suspension control, based on *MPC*, considering a *quarter-car* vehicle model and previously-measured road disturbances;
- Likewise, in [19], the proposition of a clipped-optimal control algorithm is seen, with some experimental results;
- Finally, in [20], a hybrid *MPC* controller is presented, with some strong discussion on the use of a *clipped* analytical *MPC* approach.

Considering *half-car* and other models:

- In [21], a *fast MPC* scheme is designed for a *half-car* vehicle, where the controller is tuned based on a *quarter-car* suspension model and does not take into account the effect of future disturbances;
- Finally, in [22], an *MPC* is formulated aiming safe handling performances and validated with experimental results with a 10 ms sampling period, considering a linear bicycle model and an affine force-input model.

Throughout literature, only few studies have been concerned by multivariable *MPC* semi-active control techniques considering the full car dynamics. In [23], a nonlinear programming solution approach to this problem is proposed, considering an approximate description of constraints and dependent on the use of a camera to preview future disturbances, which might not be practically implementable due to costly expenses. On the other hand, in [16], a full vehicle semi-active suspension *MPC* control is formulated and solved using Mixed Integer constraints and optimization, where simulation results show the interest of this control approach. A more detailed version, presented in [24], shows that practical implementation on a vehicle testbed is could not be achieved, since that the computational time of the *MPC* is much greater than the sampling period. It is a known fact that the computation requirements of predictive controllers (*MPC*) are usually high, due to the complex optimization problem which has to be solved **online**, at every sampling period.

1.3. Why a Linear Parameter Varying System Approach?

Thus, in this work, we will develop a practically implementable semi-active suspension *MPC* controller for a full vehicle with 4 semi-active dampers, designed in an *LPV* framework.

Indeed, an *LPV* system representation is used in this work in order to adapt the nonlinear input constraints of the dampers (dissipativity constraints) into linear constraints dependent on the scheduling parameters.

1.4. Paper's Contributions

The paper's contributions are summarized below:

- A Fast *LPV-MPC* suspension control is presented by solving a suboptimal quadratic minimization problem with polyhedral constraints, with explicit mathematical methods. The theoretical innovations of this topic reside in the proposition of a linear parameter varying (fast) predictive controller that can solve the suspension control problem in a sufficiently small computational time, allowing possible *real-time* application, which has not been seen previously in literature.

- An H_2 extended state observer is presented in order to estimate system states and disturbances. It is also used to predict future road profile disturbances. Notice that the performances of *MPC* controllers are improved with the use of accurate future disturbance information, as clearly seen in a class of applications, e.g. in [25, 26]. This is a also novel practical contribution.

- All theoretical formulation, simulation results and observer validation are presented with details, showing the interest of the proposed control approach. Comparisons with other simpler control approaches are provided in simulation, considering a full realistic nonlinear model.

The structure of this article is given as follows: Section 2 describes the *LPV* full vertical vehicle model with 4 semi-active suspensions, Section 3 presents the proposed fast *LPV MPC* controller for the semi-active suspension problem, Section 4 is devoted to the practical implementation of the control scheme, considering an extended H_2 state-observer to estimate future disturbances and system states, validated with the aid of experimental results. In Section 5, results of the global control scheme are presented and analysed in a thorough discussion. Finally, conclusions are drawn in Section 6.

2. Full LPV Vehicle Model

Firstly, this Section presents the dynamical model of a vehicle's vertical behaviour. This is a classic 7 degrees of freedom (DOF) suspension model, as seen in Figure 1 and adapted from [27]; it will be used for control design purposes. This model involves the chassis dynamics (vertical displacement (z_s), roll angle (θ) and pitch angle (ϕ)) and the vertical displacements of the wheels ($z_{us_{ij}}$) at the front/rear - left/right corners ($i = (f, r)$ and $j = (l, r)$). This $7 - DOF$ model is governed by the following equations:

$$\left.\begin{array}{rcc} m_s\ddot{z}_s & = & -F_{sfl} - F_{sfr} - F_{srl} - F_{srr} \\ I_x\ddot{\theta} & = & (-F_{sfr} + F_{sfl})t_f + (F_{srl} - F_{srr})t_r \\ I_y\ddot{\phi} & = & (F_{srr} + F_{srl})l_r - (F_{sfr} + F_{sfl})l_f \\ m_{us_{ij}}\ddot{z}_{us_{ij}} & = & F_{s_{ij}} - F_{tz_{ij}} \end{array}\right\} \quad (1)$$

where I_x and I_y represent the moments of inertia of the sprung mass around the longitudinal and lateral axis, respectively, h represents the height of the center of gravity (COG). l_f, l_r, t_f and t_r are the COG-front, rear, left and right distances, respectively.

The vertical tire forces, $F_{tz_{ij}}$, are given by:

$$F_{tz_{ij}} = k_{t_{ij}}(z_{us_{ij}} - z_{r_{ij}}) \quad (2)$$

where $k_{t_{ij}}$ are the stiffness coefficients of the tires and $z_{r_{ij}}$ are the road profile disturbances that the vehicle is subject to.

Each vertical suspension force (at 4 corners of the vehicle) is represented by $F_{s_{ij}}$ and, in this study, will be modeled by a spring and a damper with linear and nonlinear characteristics, respectively. This is:

$$\begin{array}{rcl} F_{s_{ij}} & = & k_{ij}(z_{s_{ij}} - z_{us_{ij}}) + F_{d_{ij}} \\ F_{s_{ij}} & = & k_{ij}z_{def_{ij}} + F_{d_{ij}} \end{array} \quad (3)$$

where k_{ij} represents the nominal spring stiffness coefficient, $z_{def_{ij}}$ the deflection displacement (thus, $\dot{z}_{def_{ij}}$ the deflection velocity) and $F_{d_{ij}}$ the semi-active

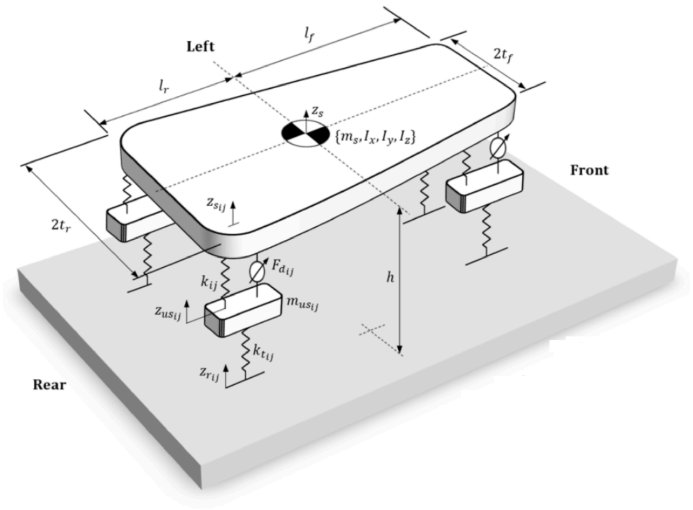

Figure 1: Full Vehicle Model with 4 Semi-Active Suspensions

the controlled damper force. This damper force is given by (4), where $c_{ij}(\cdot)$ represents controlled damping coefficient. The dissipativity constraints of each semi-active damper are formulated in (6). The feasible set within which the semi-active damper force can be applied is also illustrated by Figure 2.

$$F_{d_{ij}} = c_{ij}(\cdot)(\dot{z}_{s_{ij}} - \dot{z}_{us_{ij}}) = c_{ij}(\cdot)\dot{z}_{def_{ij}} \tag{4}$$

$$F_{d_{ij}}^{min} \leq F_{d_{ij}} \leq F_{d_{ij}}^{max} \tag{5}$$

$$0 \leq c_{min_{ij}} \leq c_{ij}(\cdot) \leq c_{max_{ij}} \tag{6}$$

The first step of the proposed LPV approach consists in rewriting the damper forces as given by (7), where u_{ij} is an incremental damping coefficient (used as control input) and $c_{nom_{ij}} = \frac{(c_{max_{ij}} + c_{min_{ij}})}{2}$ is the nominal damping coefficient. Then, the suspension force given in equation (3) can be given stated as (8). This will be useful in order to write the dissipativity constraints solely in terms of the contro inputs u_{ij}, as details Section 2.2.

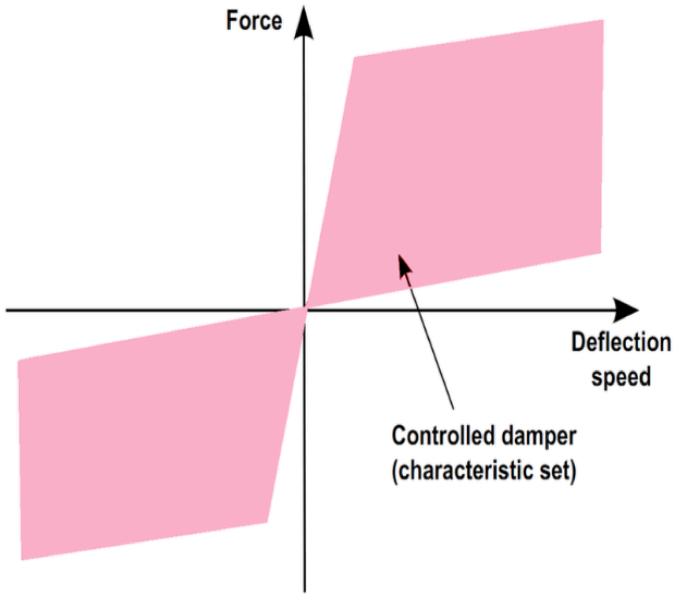

Figure 2: Semi-Active Damper: Feasible Force Region

$$F_{d_{ij}} = \overbrace{c_{nom_{ij}}(\dot{z}_{def_{ij}})}^{\text{passive}} + \overbrace{u_{ij} \times (\dot{z}_{def_{ij}})}^{\text{controlled}} \tag{7}$$

$$F_{s_{ij}} = k_{ij}(z_{def_{ij}}) + c_{nom_{ij}}(\dot{z}_{def_{ij}}) + \underbrace{u_{ij}}_{\text{control input}} \times(\dot{z}_{def_{ij}}) \tag{8}$$

Remark 1. The position (and, thus, the velocity) of the sprung mass at each corner of the vehicle ($z_{s_{ij}}$) is derived from the vehicle equations of motion, and considering the roll and pitch angles as small enough, they can be linearized as in:

$$\begin{aligned} z_{s_{fl}} &= z_s - l_f(\phi) + t_f(\theta) \\ z_{s_{fr}} &= z_s - l_f(\phi) - t_f(\theta) \\ z_{s_{rl}} &= z_s + l_r(\phi) + t_r(\theta) \\ z_{s_{rr}} &= z_s + l_r(\phi) - t_r(\theta) \end{aligned} \tag{9}$$

2.1. The Proposed LPV *State-Space Representation*

A major stride of this work in order to reduce the computational time costs of the control laws is to consider an LPV model of the full vehicle, instead of a nonlinear one. In terms of the MPC approach, this model will be considered fixed through the prediction horizon, for a given scheduling parameter, in order to compute the optimal control law. This reduces computational costs since an LPV model with a fixed scheduling parameter is, basically, Linear Time-Invariant (LTI).

To formalize the LPV parameter-dependency of the full vehicle model presented next, the following assumption is made:

Assumption 2.1. *The suspension's deflections velocities $\dot{z}_{def_{ij}}$ are bounded, due to physical limits, and can be measured or, a least, accurately estimated. As of Equation (5), one has:*

$$\frac{F_{d_{ij}}^{min}}{max\{c_{ij}(\cdot)\}} \quad \leq \quad \dot{z}_{def_{ij}} \leq \frac{F_{d_{ij}}^{max}}{min\{c_{ij}(\cdot)\}} \tag{10}$$

Then, these variables can be considered (together) as a scheduling vector Θ:

$$\begin{aligned} \Theta(t) &= diag\{\dot{z}_{def_{ij}}(t)\} \\ &= \begin{bmatrix} \dot{z}_{def_{fl}}(t) & 0 & 0 & 0 \\ 0 & \dot{z}_{def_{fr}}(t) & 0 & 0 \\ 0 & 0 & \dot{z}_{def_{rl}}(t) & 0 \\ 0 & 0 & 0 & \dot{z}_{def_{rr}}(t) \end{bmatrix} \end{aligned} \tag{11}$$

So, taking Assumption 2.1 as true, one obtains the following *state-space* representation of the Full Car model, by injecting (2) and (8) into (1). This is:

$$\sum_{Full} := \begin{cases} \dot{x}(t) = Ax(t) + B_1 w(t) + B_2(\Theta(t))u(t) \\ y(t) = Cx(t) + D_1 w(t) + D_2(\Theta(t))u(t) \end{cases} \tag{12}$$

where the system states are given by (13), the control inputs are given by (14) and the unmeasured inputs (disturbances) by (15) The measured outputs will

be detailed in Section 4.1. Matrices B_2 and D_2 are LPV and dependent on Θ, whereas A, B_1, C and D_1 are constant.

$$\begin{aligned} x &= [\ z_s \quad \theta \quad \phi \quad z_{us_{fl}} \quad z_{us_{fr}} \quad \dots \\ &\qquad z_{us_{rl}} \quad z_{us_{rr}} \quad \dot{z_s} \quad \dot{\theta} \quad \dots \\ &\qquad \dot{\phi} \quad \dot{z}_{us_{fl}} \quad \dot{z}_{us_{fr}} \quad \dot{z}_{us_{rl}} \quad \dot{z}_{us_{rr}}\ ]^T \end{aligned} \tag{13}$$

$$u = \left[\ u_{fl} \quad u_{fr} \quad u_{rl} \quad u_{rr}\ \right]^T \tag{14}$$

$$w = \left[\ z_{r_{fl}} \quad z_{r_{fr}} \quad z_{r_{rl}} \quad z_{r_{rr}}\ \right]^T \tag{15}$$

Since a Model Predictive Control approach is considered, an optimization problem will be solved at each sampling period (T_s). The continuous-time model (12) is discretized as presented in (16). Note that the matrices A_d, B_{1d}, C_d and D_{1d} are constant and matrices B_{2d} and D_{2d} are LPV.

$$\sum_{LPV}^{T_s} := \left\{ \begin{array}{rcl} x[k+1] &=& A_d x[k] + B_{1d} w[k] + B_{2d}^{\mathrm{LPV}}(\Theta) u[k] \\ y[k] &=& C_d x[k] + D_{1d} w[k] + D_{2d}^{\mathrm{LPV}}(\Theta) u[k] \end{array} \right\} \tag{16}$$

The parameter-dependency of matrices B_{2d}^{LPV} and D_{2d}^{LPV} is affine in the scheduling vector Θ, this is:

$$B_{2d}^{\mathrm{LPV}}(\Theta) = B_{2d} \times \Theta \tag{17}$$

$$D_{2d}^{\mathrm{LPV}}(\Theta) = D_{2d} \times \Theta \tag{18}$$

2.2. Input Constraints

Now, the dissipativity conditions of the semi-active suspension systems are described with more details, to cope with the MPC approach. From equations (6-7), it follows:

$$c_{min_{ij}} |\dot{z}_{def_{ij}}| \leq |F_{d_{ij}}| \leq c_{max_{ij}} |\dot{z}_{def_{ij}}| \tag{19}$$

Since $c_{nom_{ij}} = \frac{(c_{max_{ij}} + c_{min_{ij}})}{2}$, the controller will ensure:

$$\frac{(c_{min_{ij}} - c_{max_{ij}})}{2} \leq u_{ij} \leq \frac{(c_{max_{ij}} - c_{min_{ij}})}{2} \tag{20}$$

3. A Fast *LPV* Model Predictive Control Solution for Semi-Active Suspension Control

The main objective of the semi-active automotive suspensions is to isolate the body from the road disturbances, without deteriorating road handling, [5]. These two objectives can be referred to as *comfort performance* and *handling performance*, respectively, and can be described through the vehicle's *COG* acceleration (given by $\ddot{z}_s$) and roll angle (given by θ), as seen in [28].

For control design purposes, two perfomance indexes, with respect to each control objective, are considered:

$$J_{comfort} = \int_0^\tau \ddot{z}_s^2(t)dt \tag{21}$$

and

$$J_{roll} = \int_0^\tau \theta^2(t)dt \tag{22}$$

where τ represents a given time interval. Let us recall that it is well-known that (physically) these two objectives are conflicting. For this reason, the control method must take into account a suitable trade-off between these performance indexes, subject to with the input constraints given in equation (19). Moreover, one may consider a possible minimization of the chassis' displacement ($z_s(t)$), for other control purposes (this can help in terms of comfort perfomances for some road profiles).

Thus, this control problem can be solved by a well-posed constrained optimization problem, formulated within the Model Predictive Control framework. The *MPC* control approach to the semi-active suspension problem consists in minimizing the following cost function at every discrete-time step k in a computational time smaller than the sampling period T_s:

$$J(U, x[k], w, N_p) = \tag{23}$$
$$\sum_{j=1}^{N_p}[\xi_1(\frac{\ddot{z}_s[k+j|k]}{\ddot{z}_s^{\max}})^2 + \xi_2(\frac{\theta[k+j|k]}{\theta^{\max}})^2]$$
$$+\sum_{j=1}^{N_p}[\xi_3(\frac{z_s[k+j|k]}{z_s^{\max}})^2] + \sum_{j=0}^{N_p-1} u^T[k+j|k]Q_u u[k+j|k]$$

where N_p is the given prediction horizon, $u[k+j|k]$, $\ddot{z}_s[k+j|k]$, $z_s[k+j|k]$ and $\theta[k+j|k]$ denote, respectively, the control efforts, the chassis acceleration, the chassis displacement and roll angle predicted for instant $k+j$ at instant k, using the LPV prediction model (16) and considering the initial states $x[k]$ and disturbance information w.

$$U = \left[\begin{array}{cccc} u[k|k] & u[k+1|k] & \dots & u[k+N_p-1|k] \end{array} \right]^T \tag{24}$$

represents the vector of control efforts inside the prediction horizon (to be optimized). Q_u is a weighting matrix and ξ_1, ξ_2 and ξ_3 are weighting coefficients that influence the trade-off between handling and comfort performances.

Remark 2. For this application to be scale-wise correct, the control inputs u, z_s, $\ddot{z}_s$ and θ are normalized with the use of $z_s^{\max}$, $\ddot{z}_s^{\max}$ and $\theta^{\max}$ - these values are retrieved from experimentation each vehicles.

As already stated, the scheduling vector Θ is considered (for simplicity) to remain **constant** at Θ_0 during the prediction horizon, from the *MPC*'s point-of-view. This reduces computational efforts while maintaining good control performances. Thus, finally, the *LPV-MPC* design can be defined as:

$$\begin{array}{ll} \min_U & J(U, \hat{x}[k], \hat{w}, N_p, \Theta_0) \\ \text{s.t.} & \left\{ \begin{array}{c} \hat{x}[k+1] = A_d\hat{x}[k] + B_{1d}\hat{w}[k] + B_{2d}^{\text{LPV}}(\Theta_0)u[k] \\ \text{dissipativity constraints in (19)} \end{array} \right\} \end{array} \tag{25}$$

So, the two following assumptions must be satisfied.

Assumption 3.1. *The states (13) are measurable or, at least, accurately estimated.*

Assumption 3.2. *The information on the road profile disturbances, given by $\hat{w}[k]$, is available to the controller at every measurement instant k. This information can come from preview structures or adaptive schemes, like the one presented in [29]. Herein, this information will come from an extended observer, as presented later in Section 4.2.*

Remark 3. In this work, an extended observer will be used in order to estimate system states and future disturbances. This observer will be detailed next, in Section 4. Obviously, the computation of the estimated states and disturbances by this H_2 extended observer has to be done *before* the *MPC* computation in a fast-enough response time.

Considering the *MPC* control approach, the problem (25) is solved at every iteration k and the control effort to be applied to the real system corresponds to the first entry of the minimized control effort vector U, given in (24), solution to the problem (25). In Figure 3, the proposed control approach is summarized, considering the *LPV-MPC* approach.

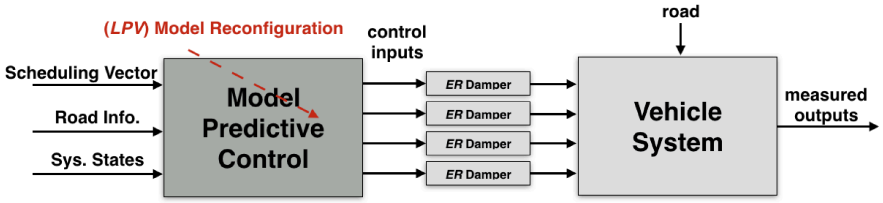

Figure 3: Proposed Predictive Control Scheme

3.0.1. Computational Time Constraints

This test-bench is able to interpret *Matlab* and *SimuLink* control laws, operating on a **fixed** sampling frequency of $f_s = 200\,\text{Hz}$. This condition is restrictive in terms of computational response time of proposed control laws, but mimics conditions of digital control systems implemented on real vehicles. Obviously, this condition implies that the available working time within which the proposed control scheme has to compute the control law is fixed and has to be **smaller** than $0.005\,\text{s}$ [1]

Through simulation, the online computation an *MPC*-based controller, as proposed in [16], was tested, with the use of *Matlab*, *Yalmip* toolbox tools [31],

[1] Note that this sampling rate is realistic and adequate for actual *top*-cars, see [30].

and *Gurobi* solver [32]. The mean computational time, considering these software packages, is around 0.0295 s. These results come from simulation on a 2.4 GHz, 8 GB *RAM Macintosh* computer, although similar values were obtained using different (top) PCs (running *Windows* and *Unix*); different solvers were also (unsuccessfully) tried. Modern automotive application make use of even tighter sampling periods, such as 1 ms, which would never be achieved with such application, as discussed in [24]. Obviously, **faster approaches had to be proposed** and this is the goal of this article.

3.1. Sub-Optimal Fast Implementation

The detailed *LPV-MPC* approach (25) will be solved with approximate sub-optimal methods, in order to fit with the maximal computing time constraint of 5 ms, and be able to be implemented in *real-time* with a microcontroller for semi-active suspension systems. This is necessary as the full constrained optimization solution overlaps the maximal allowed time, as discussed in section 3.0.1 of this paper. The approximate method that is used herein, named **Fast Model Predictive Control** (*FMPC*), was firstly introduced in [33]. Here, this method is slightly adapted to cope with the LPV model and its assumptions.

This method can compute an optimal control law, minimizing cost function (23), at every sampled instant k, even for time-varying input disturbances and space-state representation matrices - which is the case of this work, for $B_{2d}(\Theta)$ and $D_{2d}(\Theta)$ are time-varying, as well as $w(t)$. This approach is also interesting since it has been proved (in [33]) to work with a system with even 12 states, 3 control inputs and a horizon of 30 samples, computing the control actions in around 5 ms - the problem studied herein is of similar size and time constraints. The LPV model reconfiguration is described by the pseudo-code 1.

The *FMPC* method can greatly speed up the computational time of the control action. It consists in exploiting the special structure of the *MPC* quadratic problem and solving the problem approximately with the use of an early terminated *primal barrier interior-point* method combined with warm-start techniques. The quality of the achieved control is very high, as demonstrated in [33].

Algorithm 1 LPV-FMPC

Constants: T_s, A_d, B_{1d}, B_{2d}, C_d, D_{1d}, D_{2d};

for every T_s **do**

Constants: $x[k]$

Compute $\hat{w}[k]$, with model A_{mw}

Constants: $\Theta[k]$

Compute B_{2d}^{LPV}

Compute D_{2d}^{LPV}

Compute $U ==$ FMPC$(J, x, \hat{w}, \text{constraints}, A_d, B_{1d}, B_{2d}^{LPV}, C_d, D_{1d}, D_{2d}^{LPV})$

Apply $U(0)$

end for

Notice that this approach only considers linear inequality constraints on control inputs and states, which, for our control problem (using the LPV formulation) is compatible.

To be synthetic, the *FMPC* method consists in solving the *MPC* problem approximately (sub-optimal), given the following steps:

1. Rearranging the quadratic program with the use of a Primal-Barrier term, maintaining the convex optimization problem with linear equality constraints structure, where the barrier term is parametrized by factor κ;
2. Using an Infeasible Start Newton Method and a fast computation of the Newton step, considering the use of a residual vector and a search for increments solved by linear equations;
3. Using a *Schur complement* and *Cholesky* factorizations and some other simplifying techniques;
4. Finally, fixing a maximal iteration limit for the Newton algorithm and using warm start techniques, i.e. taking the previous plan of control actions ($U[k|k]$), shifted in time as the starting point for the next Newton loop.

Remark 4. As summarized by Algorithm 3.1, the *FMPC* control law obtained at each sampled instant k depends on the parameter-varying matrices B_{2d}^{LPV} and

D_{2d}^{LPV}, affine on the scheduling vector **fixed** at instant k, noted Θ_0 (considered constant throughout the prediction horizon N_p, as explained beforehand). For further reading on the stability and optimality issues of this kind of approach, and in particular on the procedure to determine bounds on the suboptimality of this *FMPC* solution, refer to [34].

The proposed *LPV-FMPC* strategy for the control of semi-active suspension system is efficiently synthesized using *Matlab*.

4. Practical Implementation

As stated before, Assumptions 3.1 and 3.2, the proposed *LPV-FMPC* controller needs to be fed with $x[k]$ and $\hat{w}[k]$ by some other scheme. To ensure the feasibility and accuracy of the control objectives, this work considers an extended observer approach to estimate system states and disturbances. Hereafter, the used experimental testbed is presented and, then, the observer design methodology.

4.1. Experimental Test-bench

In this work, an experimental platform (see Figure 4) is considered as a tool for validation in order to retrieve physical and computational constraints to the control problem, as it mimics all operational aspects of a real car.

This testbed is the *INOVE Soben-Car*, a reduced-size vehicle where several configurations and use cases can be tested (see full details in [30], [29] and on the website [35]). Table 1 gives the numerical values of the modelling parameters related to the dynamic model (12) of the *Soben-car*.

Figure 4: *INOVE Soben-Car* Test-Bench, see website [35]

Table 1: Vehicle Model Parameters: *INOVE Soben-car*

Parameter	Value	Unit
m_s	9.08	kg
$m_{us_{fl}}$	0.32	kg
$m_{us_{fr}}$	0.32	kg
$m_{us_{rl}}$	0.485	kg
$m_{us_{rr}}$	0.485	kg
I_x	5	kg.m^2
I_y	2.5	kg.m^2
t_f	0.23	m
t_r	0.23	m
l_f	0.2	m
l_r	0.37	m
$k_{t_{fl}}$	18097.60	N/m
$k_{t_{fr}}$	18097.60	N/m
$k_{t_{rl}}$	20819.40	N/m
$k_{t_{rr}}$	20819.40	N/m
k_{fl}	1396	N/m
k_{fr}	1396	N/m
k_{rl}	1396	N/m
k_{rr}	1396	N/m
$c_{max_{fl}}$	111.729	N.s/m
$c_{min_{fl}}$	31	N.s/m
$c_{max_{fr}}$	111.729	N.s/m
$c_{min_{fr}}$	31	N.s/m
$c_{max_{rl}}$	111.729	N.s/m
$c_{min_{rl}}$	31	N.s/m
$c_{max_{rr}}$	111.729	N.s/m
$c_{min_{rr}}$	31	N.s/m

On the *INOVE* testbed, the semi-active suspension system includes four Electro-Rheological (*ER*) dampers, [36], which have a force range of approximately $\pm\,20\,\mathrm{N}$. These dampers are adjusted using a controlled voltage inside the range of $[0\,,\,5]\,\mathrm{kV}$, generated by amplifier modules. The control input for these modules are *PWM* signals at $25\,\mathrm{kHz}$. A real controllable automotive suspension system has the same structure. Below each wheel lies a linear servomotor that is used to mimic the desired road profile $z_{r_{ij}}$. This servomotors have a bandwidth of $0 - 20\,\mathrm{Hz}$ and operate with a maximal velocity of $1.5\,\mathrm{m/s}$.

The real nonlinear behaviour of the *ER* semi-active dampers are seen in Figure 5, where the *Force vs. Deflection Velocity* diagram is plotted, as presented in [24]. These characteristics are related on the input constraints presented on equation (19).

This test-bench is equipped with a wide variety of sensors that capture the vehicle's behaviour. The available measured outputs (y) are given in equation (26). These measurements might also be present in a real vehicle, with the use of accelerometers and relative displacement sensors.

$$
\begin{aligned}
y \;=\; [\; & \ddot{z}_{s_{fl}} \quad \ddot{z}_{s_{fr}} \quad \ddot{z}_{s_{rl}} \quad \ddot{z}_{s_{rr}} \quad \dots \\
& z_{def_{fl}} \quad z_{def_{fr}} \quad z_{def_{rl}} \quad z_{def_{rr}} \quad \dots \\
& \dot{z}_{def_{fl}} \quad \dot{z}_{def_{fr}} \quad \dot{z}_{def_{rl}} \quad \dot{z}_{def_{rr}} \;]^T
\end{aligned}
\tag{26}
$$

4.2. H_2 Observer

Considering the presented testbed, the observer design has to take two goals into account: estimate the system's states $x[k]$ and disturbances $w[k]$ and predict the future disturbances $w[k+n]$ and states $x[k+n]$. This is depicted in Figure 6, where the complete control problem is illustrated.

To satisfy these two design goals, this work must firstly consider a disturbance model. As exploited and discussed thoroughly in [37] and [38], and since

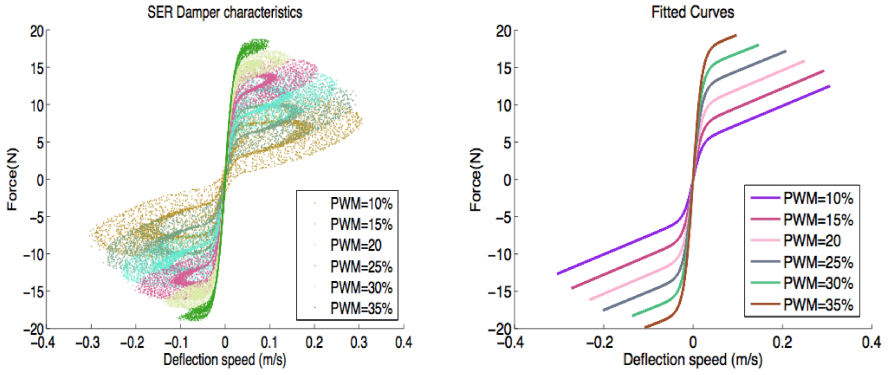

Figure 5: Force-Speed Characteristics - *ER* Semi-Active Dampers

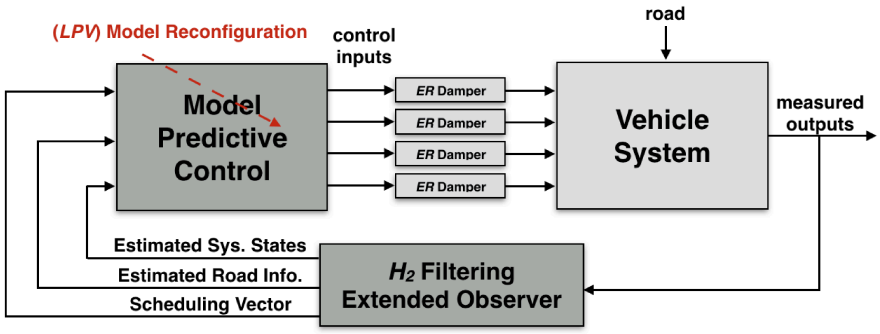

Figure 6: Proposed Predictive Control Scheme

the system model (12) has no integrating modes (considering input/output dynamics), the control perfomances can already be improved with the use of a simple constant model for disturbances. This is, considering:

$$\hat{w}[k+n] \quad = \quad w[k] \qquad \text{for} \qquad n = 1 \ldots N_p \tag{27}$$

where N_p stands for the prediction horizon.

Remark 5. Unlike [23], this method does not add any complexity in terms of sensors (no need for cameras or added structures to the plant). If some prior knowledge of the road profile is available, a more accurate model can be

computed, as seen in [1] and [29], but, for this study, it will be considered that there is no information on the type of road profile.

From this point, joining equations (16), (26) and (27), we can consider an augmented state-space representation of the system, as follows:

$$\left.\begin{array}{rcl} \begin{bmatrix} x[k+1] \\ w[k+1] \end{bmatrix} & = & \overbrace{\begin{bmatrix} A_d & B_{1d} \\ 0 & \mathbb{I} \end{bmatrix}}^{A_{obs}} \begin{bmatrix} x[k] \\ w[k] \end{bmatrix} + \overbrace{\begin{bmatrix} B_{2d}^{\mathrm{LPV}}(\Theta_0)) \\ 0 \end{bmatrix}}^{B_{obs}} F_c[k] \\ y[k] & = & \underbrace{\begin{bmatrix} C_d & D_{1d} \end{bmatrix}}_{C_{obs}} \begin{bmatrix} x[k] \\ w[k] \end{bmatrix} + D_{2d}^{\mathrm{LPV}}(\Theta_0))F_c[k] \end{array}\right\} \quad (28)$$

Remark 6. Herein $F_c(t)$ stands for the controlled part of the damper force. This is computed, for each corner of the vehicle, as a function of the control input $u_{ij}(t)$ and the suspension deflection $z_{def_{ij}}(t)$ at given computation instant k_0, as details the following equation:

$$F_{c_{ij}}[k] = u_{ij}[k] \times z^0_{def_{ij}} \quad (29)$$

The complete vector is given by:

$$F_c[k] = \begin{bmatrix} F_{ct_{fl}}[k] & F_{ct_{fr}}[k] & F_{ct_{rl}}[k] & F_{ct_{rr}}[k] \end{bmatrix}^T \quad (30)$$

Remark 7. Once again, Θ_0 stands for the scheduling vector at the instant of measurement. $z^0_{def_{ij}}$ stands for the suspension deflection at the same instant.

Let consider that the measured outputs $y[k]$ are corrupted by some measurement noises $\nu[k]$, giving:

$$y[k] = \begin{bmatrix} C_d & D_{1d} \end{bmatrix} \begin{bmatrix} x[k] \\ w[k] \end{bmatrix} + D_{2d}^{\mathrm{fixed}} F_c[k] + F_u \nu[k] \quad (31)$$

Assumption 4.1. *In this work, it is considered that there is one measurement noise for every measured output ($F_u = \mathbb{I}_8$ and $\nu \in \mathbb{R}^8$).*

Then, one wishes to design an observer to estimate the extended states with the following structure:

$$\left.\begin{array}{rcl} \begin{bmatrix} \hat{x}[k+1] \\ \hat{w}[k+1] \end{bmatrix} & = & A_{obs} \begin{bmatrix} \hat{x}[k] \\ \hat{w}[k] \end{bmatrix} + B_{obs} F_c[k] + L(y[k] - \hat{y}[k]) \\ \hat{y}[k] & = & C_{obs} \begin{bmatrix} \hat{x}[k] \\ \hat{w}[k] \end{bmatrix} + D_{2d}^{\text{fixed}} F_c[k] \end{array}\right\} \quad (32)$$

where $L \in \mathbb{R}^{18\times 8}$ is the observer matrix gain to be defined.

To compute this gain, this work considers a classic H_2 filtering observer, with pole placement definition, as in [39]. This is an appropriate method to reduce the effect of noise on the estimations. Remark that the H_2 norm is related to the impulse to energy gain.

The estimation error dynamics of the observer are presented below:

$$e[k+1] = (A_{obs} - LC_{obs})e[k] - LF_u\nu[k] \quad (33)$$

Definition 4.2. The (discrete-time) H_2 observer problem (detailed in [39]), is, to find L in order to minimize γ such that:

$$||T_{e\nu}(z)||_2 \leq \gamma \quad \text{under} \quad e[k=0] = 0 \quad (34)$$

under

$$\lim_{k\to\infty} e[k] \to 0 \quad \text{for} \quad \nu[k] \equiv 0 \quad (35)$$

where $T_{e\nu}(z)$ stands for the (z-domain) transfer function that represents the effects of $\nu(z)$ upon the estimation error:

$$e(z) = \begin{bmatrix} x(z) \\ w(z) \end{bmatrix} - \begin{bmatrix} \hat{x}(z) \\ \hat{w}(z) \end{bmatrix} \quad (36)$$

In order to improve the convergence performances of the observer, this work considers an additional constraint concerning the poles of the computed observer which are to be placed inside a parameterized region $\mathcal{R}_p(\mu, \varrho)$ (circle centered at μ with radius ϱ), smaller than the unit circle (being fast enough for the semi-active suspension problem's goals), as depicted in Figure 7.

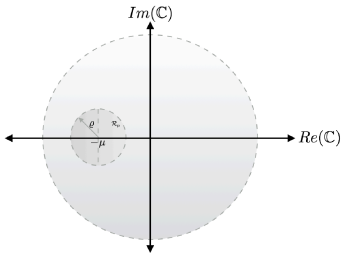

Figure 7: H_2 Observer: Pole Placement Region

Lemma 4.3. *Consider the system's model (28) and (31) with observer (32). As seen in [40], the problem solution is minimize γ such that there exists two positive definite symmetric matrices P and R and a block matrix Y so that the following Linear Matrix Inequalities hold:*

$$\begin{bmatrix} P & P(\frac{A_{obs}-\mu\mathbb{I}}{\varrho}) - Y\frac{C_{obs}}{\varrho} & -Y \\ \star & P & 0 \\ \star & \star & \mathbb{I} \end{bmatrix} > 0,$$
$$\begin{bmatrix} R & \mathbb{I} & 0 \\ \star & P & 0 \\ \star & \star & \mathbb{I} \end{bmatrix} > 0, \tag{37}$$
$$Trace(R) < \gamma$$

From this, the observer matrix gain L is computed as $L = P^{-1}Y$.

Now, let present the numerical values of the H_2 filtering observer design: for the studied control application, the computation of the *LMI*s yields $\gamma = 0.6602$, which leads to a good observer, considering $\varrho = 0.03$ and $\mu = 0.0067$. This solution was obtained with the use of *MATLAB*, and the solver *SeDuMi* [41].

4.3. Experimental Results

Some experimental validation results are presented below, depicting states (x) and road profile (disturbances, w) estimation by the designed H_2 filtering observer. These results represent a validation of the described H_2 observer, for they use real measurement data (y) retrieved from the *INOVE Soben-Car*

mechatronic testbed, considering a sequence of bumps road profile scenario z_r at each corner. The measurement noise is, naturally, present for each measured output (y).

Remark 8. There is a **trade-off** between the convergence speed of this H_2 observer (given by the pole placement region $\mathcal{R}_p(\mu, \varrho)$) and the noise-attenuation goals.

To further reject high-frequency noises, the measured outputs $y(t)$ are numerically filtered. The continuous-time transfer function of the used filter is given by:

$$W_e(s) = \frac{1}{0.001s + 1} \times \mathbb{I}_{12} \tag{38}$$

The validation scenario is that of a vehicle running at 120 km/h in a straight line on a dry road, when it encounters a sequence of 1 cm sinusoidal bumps.

Figure 8 shows an accurate estimation of the road profile at each corner of the vehicle. A *zoom* of the road profile estimation for the front-left corner is showed in details in Figure 9: the effect of the measurement noise is still present, but the main trend is followed by the estimated augmented states, which is enough from the *FMPC* controller's point-of-view.

Figure 10 displays the (sufficiently) accurate estimation of some (important) system states (pitch $\phi(t)$ and roll $\theta(t)$). Once again, the effect of $\nu(t)$ is still present (but diminished) and the main trend is followed by the estimated states.

Show by the previous Figures, the proposed H_2 filtering extended observer approach can serve well in order to provide the design controller information on states and disturbances.

5. Results, Analysis and Discussion

Simulation results are presented and discussed, considering the problem of controlling a Full Vehicle's Semi-Active Suspension, within the Model Predictive Control framework.

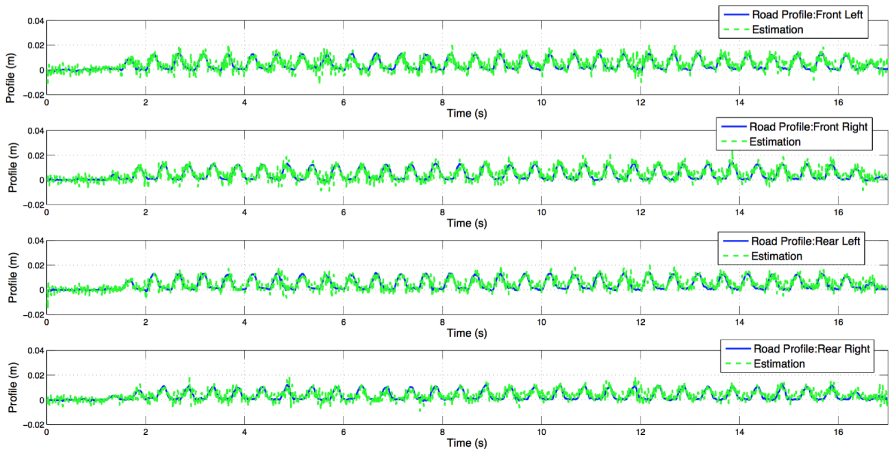

Figure 8: Road Profile Estimation by H_2 Observer

In order to improve to truthfulness of the simulations, bringing them closer to realistic conditions, the following simulation results consider a full nonlinear vehicle model, as described in [27, 42]. This model includes nonlinear suspension forces and has been validated with a real car. In order to mimic measurement noise, a high-frequency signal ($\nu(t)$) is added to each component of $y(t)$.

Considering the use of the *ER* dampers, the semi-active damper forces, given by $F_{d_{ij}}(t)$, will be treated with the use of a parametric model, adapted from [43], once again divided into passive and controlled parts:

$$F_{d_{ij}}(t) = \overbrace{f_c d_{c_{ij}}(t)\tanh(a_1 \dot{z}_{def_{ij}}(t) + a_2 z_{def_{ij}}(t))}^{\text{controlled}} + \underbrace{c_{nom_{ij}} \dot{z}_{def_{ij}}}_{\text{passive}} \tag{39}$$

where $d_c(t)$ is a controlled PWM signal (duty-cycle), given inside the set $[10\,,\,35]\,\%$. This model considers the effect of hysteresis as well as the main nonlinearities from the *ER* dampers (characteristics given by Figure 5).

In terms of simulation, each $d_{c_{ij}}(t)$ is computed as a function of $z_{def_{ij}}(t)$, $\dot{z}_{def_{ij}}(t)$ and the computed control law $u_{ij}(t)$, with the use of a statical three-

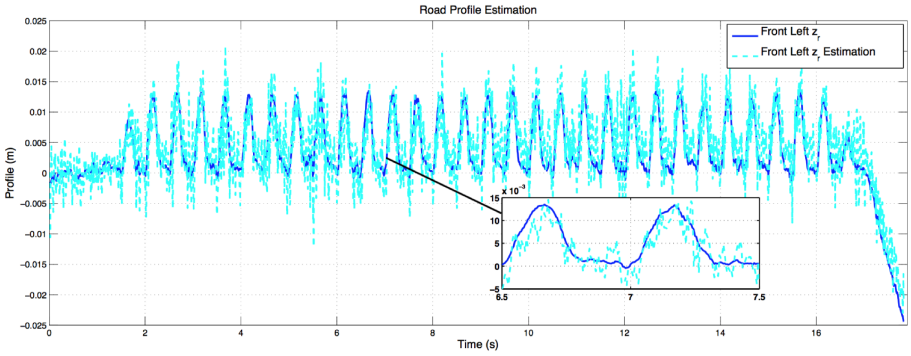

Figure 9: Front Left Road Profile Estimation by H_2 Observer

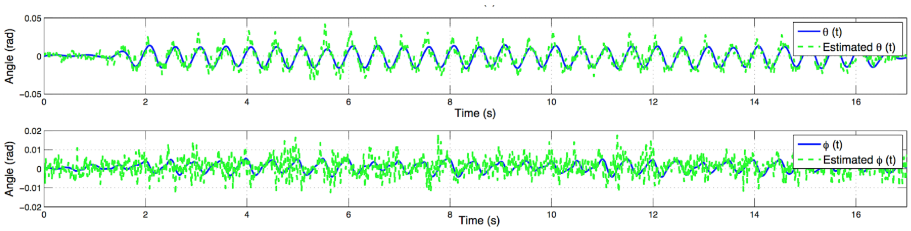

Figure 10: System States Estimation by H_2 Observer

dimensional map. This map is, obviously, given by an inverse function of (39), that depends on $z_{def_{ij}}$ and $\dot{z}_{def_{ij}}$, as represented below, in equation (40).The parameters used in equation (39) are given in Table 2.

$$d_{c_{ij}}(t) \quad = \quad \mathcal{F}(u_{ij}(t), z_{def_{ij}}, \dot{z}_{def_{ij}}) \tag{40}$$

In Figure 11, a block scheme details how the simulation of a realistic vehicle model is implemented in this work. Notice how the *MPC* controller computes the control law $u[k]$, which is converted into *PWM* signals $d_c(t)$ to be, then, applied to the *ER* damper model and the nonlinear vehicle plant.

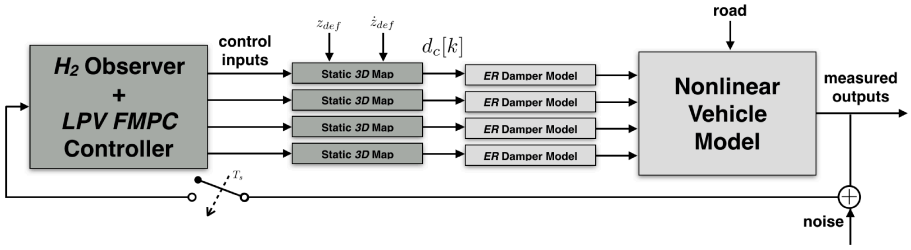

Figure 11: Complete Realistic Simulation Scheme

Table 2: Semi-Active *ER* Damper Parameters

Parameter	Value	Unit
f_c	6.5137	N
a_1	27.7154	s/m^2
a_2	1.3297	1/m

5.1. Computational Time

Before presenting practical results, let mention that the computational time constraints of the problem (as exposed on subsection 3.0.1) are **strictly** satisfied with the described Fast *MPC* solution. Through simulation, the online computation of the *FMPC* approach was tested, with the aid of software packages *Matlab* and *Yalmip* toolbox, [31]. Considering that the computational time of the H_2 extended observer is embedded into the controller's computational time, the average computational time was of 2.975 ms, which is, obviously, much smaller than the fixed sampling period (5 ms).

5.2. Simulation Results

In the following subsections, two different simulation results will be presented, in order to demonstrate that the trade-off between handling and comfort performances of the vehicle (given by cost functions (22) and (21), respectively) is efficiently achieved with the proposed Linear Parameter Varying Fast Model Predictive Control (*LPV-FMPC*) design framework.

For both simulations, the *FMPC* synthesis considered 17 as the maximal number of Newton iteration steps and the parameter κ, related to the primal-barrier term, is taken as 0.01. The prediction horizon is fixed at $N_p = 10$ samples for all the controllers; several different prediction horizons were tested by authors and these values were found to give a sufficiently good trade-off between computational time and accuracy of computed control law.

In order to compare the effectiveness of this work's propositions, the following results compare three different behaviours:

- The proposed *LPV-FMPC* approach;
- The purely passive, uncontrolled damper ($u_{ij} = 0$);
- A clipped analytical *MPC* (*AMPC*) scheme, as discussed similarly in [19].

This *AMPC* stands for the analytical, offline solution of quadratic problem (25), without taking into account the dissipativity constraints and considering the scheduling parameter $\Theta[k]$ as fixed through the horizon. The resulting control law is clipped (saturation) inside the feasible region (determined by the dampers' dissipativity constraints) and then applied to the vehicle. The use of an *Anti-Windup* gain (K_{AW}) is considered in order to unload excessive integral action. This control method is a good comparison to the *LPV-FMPC* method for it can be, also, implemented in *real-time*, given that the control law at each instant k is a simple clipped state-feedback law $u[k] = \text{clip}\{-K_x\hat{x}[k] - K_w\hat{w}[k]\}$ (anti-windup action is omitted). The matrices K_{AW}, K_x and K_w are constant and were computed offline. This approach is more robust than a simple state-feedback action because it considers the feasible region of u.

Remark 9. Although the goal of this work is not to demonstrate that the proposed *LPV-FMPC* method for Semi-Active suspensions presents better results than when using purely passive suspensions, this is illustrated by the "uncontrolled damper" results, in the following Figures.

5.2.1. Simulation Scenario 1

For the first simulation, the vehicle is running at 120 km/h in a straight line on a dry road, when a first 5 cm bump occurs simultaneously on all wheels, at time $t = 0.2$ s to excite the bounce motion and chassis vibration, a second 5 cm bump occurs, at time $t = 2$ s, but only on the left wheels, to cause a roll motion and, finally, a third bump occurs at time $t = 7$ s, at both front wheels, causing a pitch motion. To use a sequence of bumps is a classical way to deal with the analysis vertical suspension systems, given that one is able distinguish bound, pitch and roll motion, as suggests [44].

This road profile and its estimation by the H_2 observer are shown in Figure 12. Let remember that a high-frequency measurement noise was added to each measured output (y): its effect is, clearly, diminished.

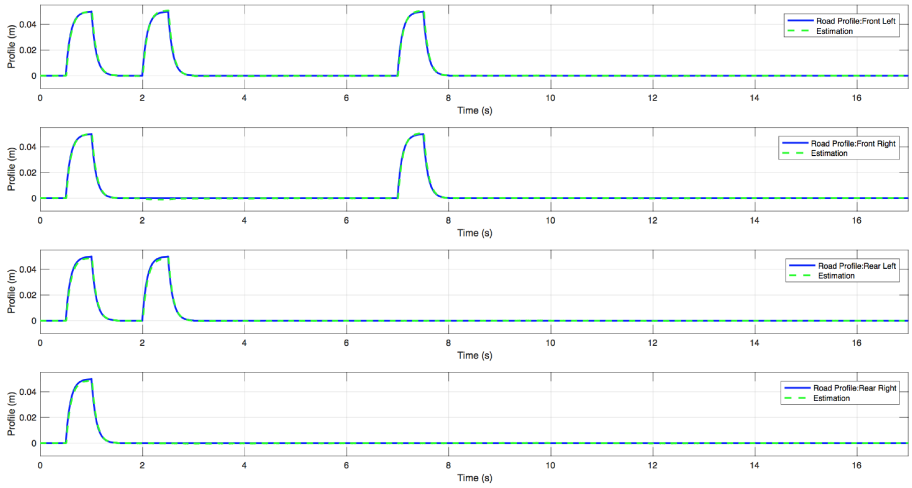

Figure 12: Road Profile and its Estimation

The scalar weighting coefficients used for the predictive controller are given in Table 3. These are settled so that the minimization of the chassis' acceleration is prioritized, while not neglecting the minimization of the roll angle, which gives a suitable trade-off, leading mainly to comfort performances of the vehicle.

Table 3: *MPC* Synthesis Parameters

Parameter	Value
ξ_1	0.975
ξ_2	0.025
ξ_3	0.00001
Q_u	$\begin{bmatrix} 0.975 & 0 & 0 & 0 \\ 0 & 0.975 & 0 & 0 \\ 0 & 0 & 0.975 & 0 \\ 0 & 0 & 0 & 0.975 \end{bmatrix}$

The chassis' displacement due to the road profile is displayed in Figure 13, for both the described control approaches and the nominal damper case. The minimization of $z_s(t)$ is not of great importance for this study, as explained beforehand.

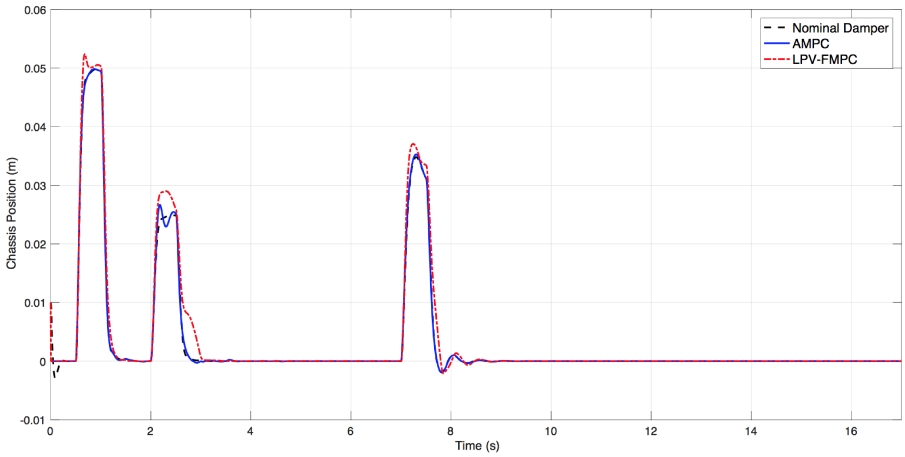

Figure 13: Chassis' Displacement, $z_s(t)$

Of uttermost importance for this simulation scenario we can see in Figure 14 the behaviour of the chassis' acceleration ($\ddot{z}_s(t)$, key for comfort performances of a vehicle) due to the road profile, with a comparison between the *AMPC*,

LPV-FMPC and the nominal damper case. As expected, in most situations the response with a controlled damper is more efficient than with a passive nominal suspension system. In Table 4, the *RMS* values (root mean square over simulation time) for these three cases are given[2]. It is thus clear that the *LPV-FMPC* method is the most efficient (specially considering what happens to the roll angle behaviour with the *AMPC* approach).

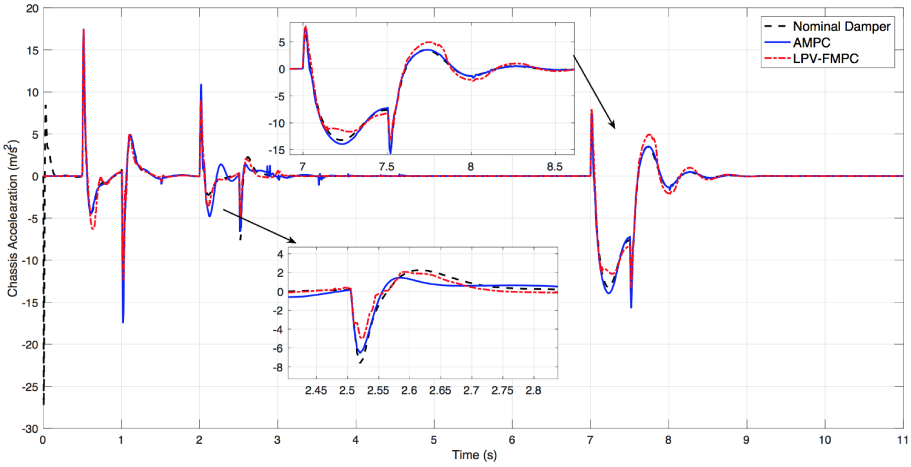

Figure 14: Chassis' Acceleration, $\ddot{z}_s(t)$

[2]The initial stabilization (due to initial conditions) has been neglected for calculus, so the *RMS* values were computed from 0.2 s onwards.

Table 4: *RMS* Values - Scenario 1

Comfort Performance - $\ddot{z}_s(t)$	Value	Unit
Uncontrolled Damper	2.22066	$\mathrm{m/s^2_{RMS}}$
AMPC	2.11640	$\mathrm{m/s^2_{RMS}}$
LPV-FMPC	2.10061	$\mathrm{m/s^2_{RMS}}$
Roll Performance - $\theta(t)$		
Uncontrolled Damper	0.2571	$\mathrm{rad_{RMS}}$
AMPC	0.2713	$\mathrm{rad_{RMS}}$
LPV-FMPC	0.2571	$\mathrm{rad_{RMS}}$

As expected, the behaviour of the vehicle's roll angle is enhanced, due to the sideways bump of the road profile around $t = 2\,\mathrm{s}$. Figure 15 shows the behaviour of the roll angle ($\theta(t)$) considering the nominal passive damper (uncontrolled, taking $u_{ij} = 0$), and a controlled semi-active damper with the *AMPC* and *LPV-FMPC* approaches. In terms of handling performances, the *LPV-FMPC* controlled response is, at least, equivalent to the nominal damper, whereas the *AMPC* controlled response is much worse, because closed-loop system might present internal instabilities (marginal stability) due to the saturation effects (clipping constraints) not taken into account during the design step. This is confirmed by the *RMS* values for $\theta(t)$, given in in Table 4.

Finally, Figure 16 clearly shows that the dissipativity constraints of all the four dampers are respected by both *Real-Time MPC*-based approaches, although, for the *AMPC* method, the controlled damping coefficient stays most of the time "forced" at $c_{max_{ij}}$ (saturation). Considering the *LPV-FMPC* method, a wider range of values of $c_{ij}(\cdot)$ is used. Figure 17 emphasizes the respective *PWM* signals to be applied to the vehicle, for both control approaches, considering the three dimensional look-up table method described.

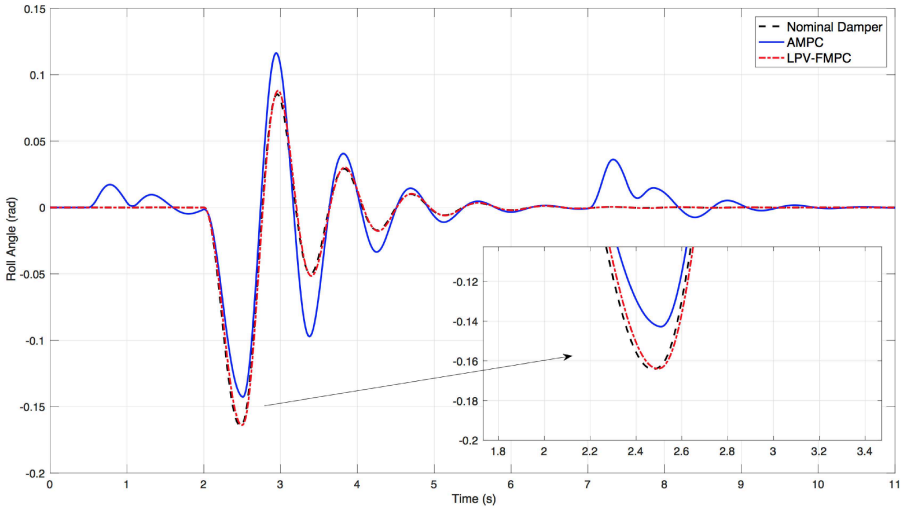

Figure 15: Roll Angle θ

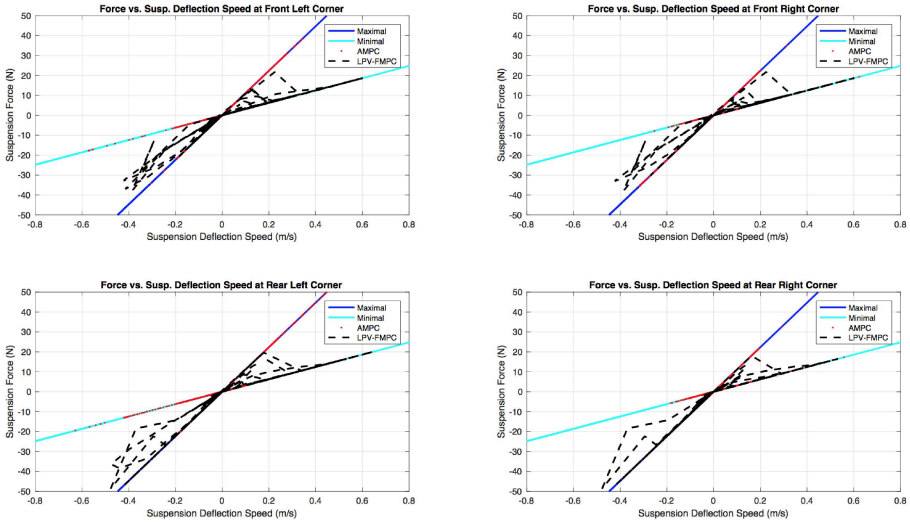

Figure 16: Suspension Force at Each Corner, $F_d(t)$

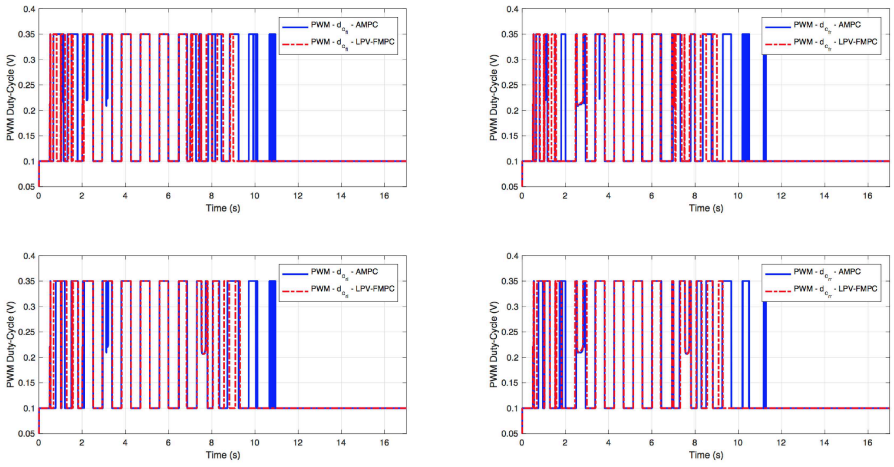

Figure 17: *PWM* Signal for Each Damper

5.2.2. *Simulation Scenario* 2

This second simulation scenario is oriented towards roll performances. A new road profile is used (see Figure 18), in order to further excite roll motion, and measurement noise are considered, but the tuning parameters for the *MPC* cost function are changed in order to prioritize the minimization of J_{roll}, as shows Table 5.

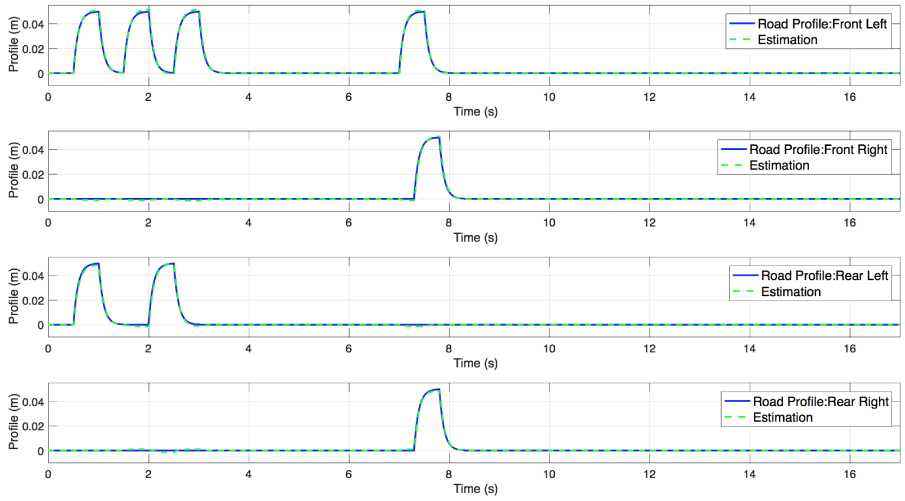

Figure 18: Simulation Scenario 2: Road Profile and its Estimation

Table 5: *MPC* Synthesis Parameters: Second Scenario

Parameter	Value
ξ_1	0.1
ξ_2	0.9
ξ_3	0
Q_u	$\begin{bmatrix} 0.9 & 0 & 0 & 0 \\ 0 & 0.9 & 0 & 0 \\ 0 & 0 & 0.9 & 0 \\ 0 & 0 & 0 & 0.9 \end{bmatrix}$

For this second scenario, the chassis' displacement behaviour is presented in Figure 19 and its acceleration in Figure 20. Clearly, once again, the *LPV-FMPC* method still outperforms the uncontrolled damper and the *AMPC* method in terms of comfort performances; as seen in Table 6.

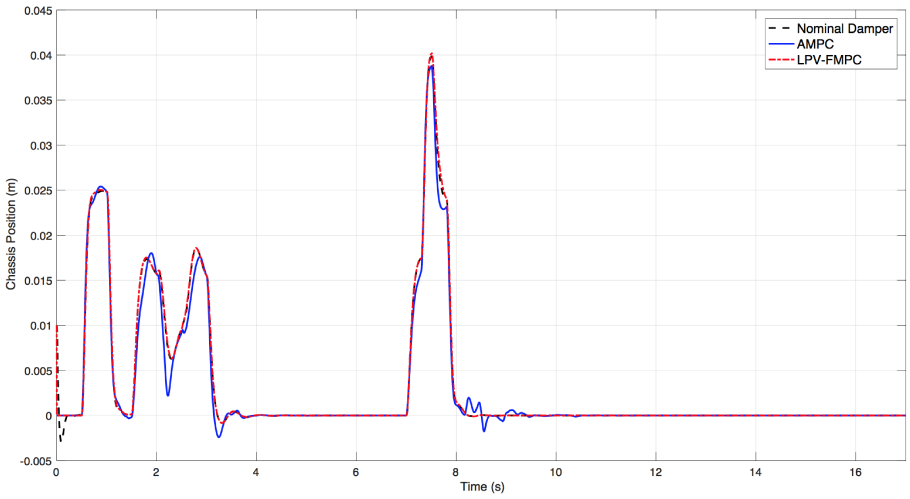

Figure 19: Chassis' Displacement - Scenario 2

Finally, as this scenario considers mostly handling performances, one should carefully analyse the roll angle behaviour, with the *AMPC* and the *LPV-FMPC*

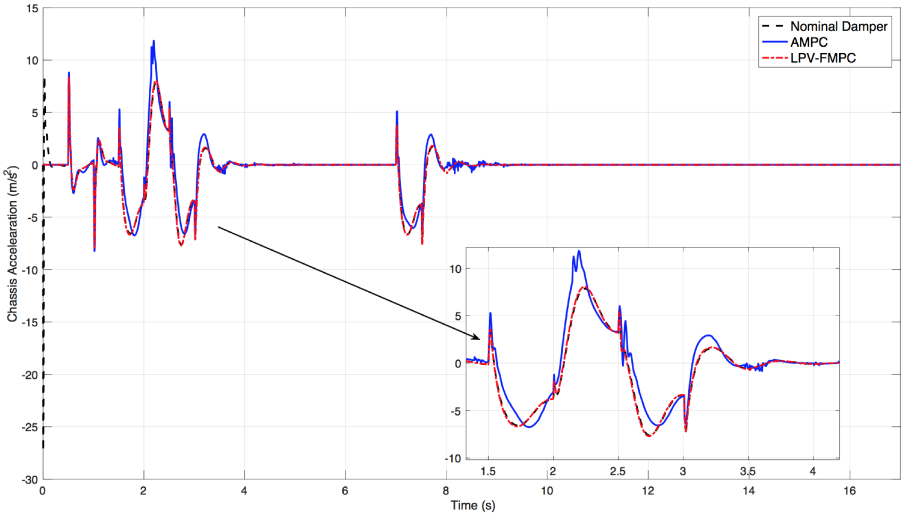

Figure 20: Chassis' Acceleration - Scenario 2

control methods and with an uncontrolled damper, given in Figure 21. Clearly, the *AMPC* method presents some internal stability issues due to the saturation (clipping) effects on the control law, which causes some unwanted oscillations, bigger than in situations with an uncontrolled damper. The *LPV-FMPC* approach, on the other hand, minimizes well $\theta(t)$, compared to the uncontrolled damper case. Once again, analyzing the *RMS* values for $\theta(t)$, Table 6 emphasizes the efficiency of the *LPV-FMPC* method.

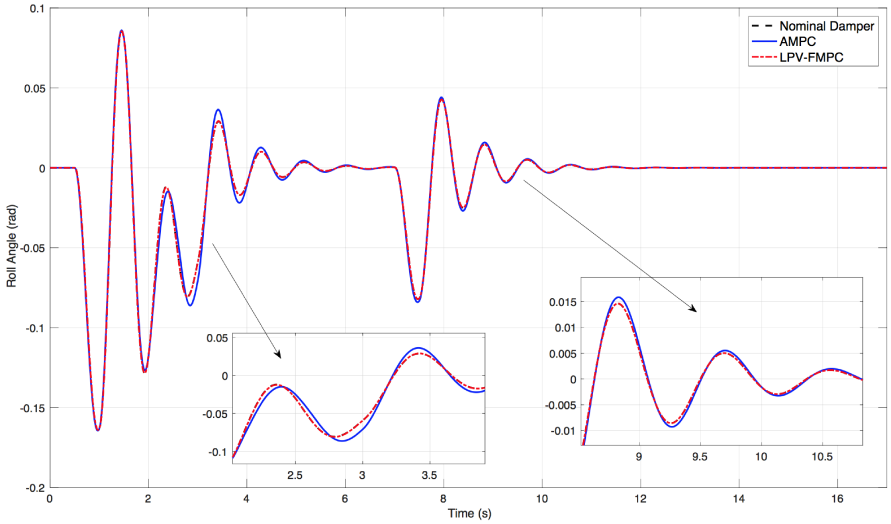

Figure 21: Roll Angle θ - Scenario 2

Table 6: *RMS* Values - Scenario 2

Comfort Performance - $\ddot{z}_s(t)$	Value	Unit
Uncontrolled Damper	1.8985	$\mathrm{m/s^2_{RMS}}$
AMPC	1.9239	$\mathrm{m/s^2_{RMS}}$
LPV-FMPC	1.8980	$\mathrm{m/s^2_{RMS}}$
Roll Performance - $\theta(t)$		
Uncontrolled Damper	$35.197.10^{-3}$	$\mathrm{rad_{RMS}}$
AMPC	$35.765.10^{-3}$	$\mathrm{rad_{RMS}}$
LPV-FMPC	$35.184.10^{-3}$	$\mathrm{rad_{RMS}}$

5.3. Final Discussion

After detailing the behaviour of the closed-loop system (as presented in Figure 3), the efficiency of the proposed LPV model-based fast predictive control approach can be discussed more deeply, given that it aims to be implemented on a real vehicle system, in the near future.

Firstly, remark that the improvements from the new proposed scheme (LPV-$FMPC$) are not huge because when compared with the nominal damper because this is a reduced (small) vehicle. Small changes in $\ddot{z}_s$ do influence the passager's comfort, just as small changes in θ influence the car's roll motion. Using a large vehicle model, the order of magnitude of $\ddot{z}_s$ and θ would greatly enlarge and the improvements would be further noticeable.

Also, remark that the $AMPC$ method is essentially used for comparison goals for it is a feasible way to implement a real-time MPC-based method for the semi-active suspension control of a full vehicle. Moreover, remark that there is no guarantee that the closed-loop system would remain stable with this $AMPC$ approach, since the saturation (clipping) phase might affect the internal stability. This is seen in terms of handling performances, as the $AMPC$ presents a behaviour ever worse than that of the uncontrolled damper. In Figure 17, one can also see that the PWM signal, with this control approach, continues to vary after the road profile stabilizes, trying to stabilize internal modes.

The trade-off between handling and comfort performances is the main goal of this work. As it was seen, for the first simulation scenario, the tuning parameters ξ were set so that the comfort performances tended to be prioritized and that the handling performance would be, at least, equivalent to the ones obtained with a passive damper. For the second simulation scenario, the tuning parameters were set in a "inverse" way, so that handling performance were prioritized.

The proposed LPV-$FMPC$ control approach presents extremely efficient results, abiding to constraints, guaranteeing internal stability (as expected) and being able to enhance comfort performances ($\ddot{z}_s$ is well minimized, compared to the uncontrolled damper behaviour) while maintaining good roll performances ($\ddot{\theta}$ is, at least, as small as when the damper is passive). The tuning parameters

can be adjusted so that an adequate trade-off is achieved, as shown through the two different simulation scenarios.

6. Conclusion and Future Works

This article presented the control of a *semi-active* suspension system, considering a full vertical vehicle model and using a fast model-based predictive control framework. A *fast* Linear Parameter Varying *MPC* control scheme is developed for a *real-time* application with a sampling frequency of 200 Hz and tested through realistic simulation scenarios, considering nonlinearities and measurement noise. An H_2 observer is designed to estimate the system states and future road disturbances, considering the attenuation of measurement noise. Thanks to the *MPC*-based strategy, a multi-objective problem is considered, implementing an efficient trade-off between road handling and passenger comfort, while ensuring dissipativity constraints, with an adequate choice of tuning parameters. The performances of the proposed *LPV-FMPC* have been assessed using simulation and compared with an analytical, unconstrained *MPC*, [19].

For further works, an interesting theme is to study different kinds of implementations of this *MPC* proposition, considering the use of Mixed Integer Quadratic Programming in *Real-Time MPC* controllers.

Acknowledgements

This work has been partially supported by the *LabEx PERSYVAL-Lab* ($ANR-11-LABX-0025-01$), funded by the French program *Investissements dávenir*. The authors also thank *CAPES* for financing project *BRAFITEC ECoSud*.

References

[1] A. Unger, F. Schimmack, B. Lohmann, R. Schwarz, Application of LQ-based semi-active suspension control in a vehicle, Control Engineering Practice 21 (12) (2013) 1841–1850.

[2] D. Hrovat, Survey of advanced suspension developments and related optimal control applications, Automatica 33 (10) (1997) 1781–1817.

[3] J. Lu, M. DePoyster, Multiobjective optimal suspension control to achieve integrated ride and handling performance, IEEE Transactions on Control Systems Technology 10 (6) (2002) 807–821.

[4] D. Fischer, R. Isermann, Mechatronic semi-active and active vehicle suspensions, Control engineering practice 12 (11) (2004) 1353–1367.

[5] S. M. Savaresi, C. Poussot-Vassal, C. Spelta, O. Sename, L. Dugard, Semi-active suspension control design for vehicles, Elsevier, 2010.

[6] C. Poussot-Vassal, C. Spelta, O. Sename, S. M. Savaresi, L. Dugard, Survey and performance evaluation on some automotive semi-active suspension control methods: A comparative study on a single-corner model, Annual Reviews in Control 36 (1) (2012) 148–160.

[7] H. E. Tseng, D. Hrovat, State of the art survey: active and semi-active suspension control, Vehicle system dynamics 53 (7) (2015) 1034–1062.

[8] H. Du, K. Y. Sze, J. Lam, Semi-active h_∞ control of vehicle suspension with magneto-rheological dampers, Journal of Sound and Vibration 283 (3) (2005) 981–996.

[9] A.-L. Do, O. Sename, L. Dugard, An LPV control approach for semi-active suspension control with actuator constraints, in: American Control Conference (ACC), 2010, IEEE, 2010, pp. 4653–4658.

[10] C. Poussot-Vassal, O. Sename, L. Dugard, P. Gaspar, Z. Szabo, J. Bokor, A new semi-active suspension control strategy through LPV technique, Control Engineering Practice 16 (12) (2008) 1519–1534.

[11] M. Q. Nguyen, J. G. da Silva, O. Sename, L. Dugard, A state feedback input constrained control design for a 4-semi-active damper suspension system: a quasi-LPV approach, IFAC-PapersOnLine 48 (14) (2015) 259–264.

[12] E. F. Camacho, C. B. Alba, Model predictive control, Springer Science & Business Media, 2013.

[13] M. M. Morato, P. R. da Costa Mendes, J. E. Normey-Rico, C. Bordons, Optimal operation of hybrid power systems including renewable sources in the sugar cane industry, IET Renewable Power Generation 11 (8) (2017) 1237–1245.

[14] F. Xu, V. Puig, C. Ocampo-Martinez, S. Olaru, S.-I. Niculescu, Robust MPC for actuator-fault tolerance using set-based passive fault detection and active fault isolation, International Journal of Applied Mathematics and Computer Science 27 (1) (2017) 43–61.

[15] R. McCloy, J. De Doná, M. Seron, Sensor switching fault tolerant MPC for constrained LPV systems, in: Decision and Control (CDC), 2017 IEEE 56th Annual Conference on, IEEE, 2017, pp. 6377–6382.

[16] M. Nguyen, M. Canale, O. Sename, L. Dugard, A model predictive control approach for semi-active suspension control problem of a full car, in: Decision and Control (CDC), 2016 IEEE 55th Conference on, IEEE, 2016, pp. 721–726.

[17] T. Van der Sande, I. Besselink, H. Nijmeijer, Rule-based control of a semi-active suspension for minimal sprung mass acceleration: design and measurement, Vehicle System Dynamics 54 (3) (2016) 281–300.

[18] C. Poussot-Vassal, S. M. Savaresi, C. Spelta, O. Sename, L. Dugard, A methodology for optimal semi-active suspension systems performance evaluation, in: Decision and Control (CDC), 2010 49th IEEE Conference on, IEEE, 2010, pp. 2892–2897.

[19] P. Brezas, M. C. Smith, W. Hoult, A clipped-optimal control algorithm for semi-active vehicle suspensions: Theory and experimental evaluation, Automatica 53 (2015) 188–194.

[20] N. Giorgetti, A. Bemporad, H. E. Tseng, D. Hrovat, Hybrid model predictive control application towards optimal semi-active suspension, International Journal of Control 79 (05) (2006) 521–533.

[21] M. Canale, M. Milanese, C. Novara, Semi-active suspension control using fast model-predictive techniques, IEEE Transactions on control systems technology 14 (6) (2006) 1034–1046.

[22] C. E. Beal, J. C. Gerdes, Model predictive control for vehicle stabilization at the limits of handling, IEEE Transactions on Control Systems Technology 21 (4) (2013) 1258–1269.

[23] C. Gohrle, A. Schindler, A. Wagner, O. Sawodny, Model predictive control of semi-active and active suspension systems with available road preview, in: Control Conference (ECC), 2013 European, IEEE, 2013, pp. 1499–1504.

[24] M. Q. Nguyen, LPV approaches for modelling and control of vehicle dynamics: application to a small car pilot plant with ER dampers, Ph.D. thesis, Université Grenoble Alpes (2017).

[25] A. Pawlowski, J. L. Guzmán, F. Rodríguez, M. Berenguel, J. E. Normey-Rico, Predictive control with disturbance forecasting for greenhouse diurnal temperature control, IFAC Proceedings Volumes 44 (1) (2011) 1779–1784.

[26] J. D. Vergara-Dietrich, M. M. Morato, P. R. Mendes, A. A. Cani, J. E. Normey-Rico, C. Bordons, Advanced chance-constrained predictive control for the efficient energy management of renewable power systems, Journal of Process Controldoi:https://doi.org/10.1016/j.jprocont.2017.11.003.

[27] C. Poussot-Vassal, O. Sename, L. Dugard, P. Gaspar, Z. Szabo, J. Bokor, Attitude and handling improvements through gain-scheduled suspensions and brakes control, Control Engineering Practice 19 (3) (2011) 252–263.

[28] U. Kiencke, L. Nielsen, Automotive control systems: for engine, driveline, and vehicle (2000).

[29] J. C. Tudón-Martínez, S. Fergani, O. Sename, J. J. Martinez, R. Morales-Menendez, L. Dugard, Adaptive road profile estimation in semiactive car suspensions, IEEE Transactions on Control Systems Technology 23 (6) (2015) 2293–2305.

[30] C. Vivas-Lopez, D. H. Alcántara, M. Q. Nguyen, S. Fergani, G. Buche, O. Sename, L. Dugard, R. Morales-Menéndez, INOVE: a testbench for the analysis and control of automotive vertical dynamics, in: 14th International Conference on Vehicle System Dynamics, Identification and Anomalies (VSDIA 2014), 2014.

[31] J. Lofberg, Yalmip: A toolbox for modeling and optimization in matlab, IEEE International Symposium on Computer Aided Control Systems Design (2004) 284–289doi:10.1109/CACSD.2004.1393890.

[32] G. Optimization, et al., Gurobi optimizer reference manual, URL: http://www. gurobi. com 2 (2012) 1–3.

[33] Y. Wang, S. Boyd, Fast model predictive control using online optimization, IFAC Proceedings Volumes 41 (2) (2008) 6974–6979.

[34] T. Besselmann, J. Lofberg, M. Morari, Explicit MPC for LPV systems: Stability and optimality, IEEE Transactions on Automatic Control 57 (9) (2012) 2322–2332.

[35] INOVE: Integrated approach for observation and control of vehicle dynamics, http://www.gipsa-lab.fr/projet/inove/index.html, accessed: 13/10/2016 (2010).

[36] R. Stanway, J. Sproston, N. Stevens, Non-linear modelling of an electro-rheological vibration damper, Journal of Electrostatics 20 (2) (1987) 167–184.

[37] A. Núñez-Reyes, J. E. Normey-Rico, C. Bordons, E. F. Camacho, A smith predictive based MPC in a solar air conditioning plant, Journal of Process control 15 (1) (2005) 1–10.

[38] A. Pawlowski, J. Guzmán, J. Normey-Rico, M. Berenguel, Improving feedforward disturbance compensation capabilities in generalized predictive control, Journal of Process Control 22 (3) (2012) 527–539.

[39] K. Zhou, J. C. Doyle, K. Glover, et al., Robust and optimal control, Vol. 40, Prentice hall New Jersey, 1996.

[40] M. J. Khosrowjerdi, R. Nikoukhah, N. Safari-Shad, A mixed h_2/h_∞ approach to simultaneous fault detection and control, Automatica 40 (2) (2004) 261–267.

[41] J. F. Sturm, Using sedumi 1.02, a matlab toolbox for optimization over symmetric cones, Optimization methods and software 11 (1-4) (1999) 625–653.

[42] S. Fergani, L. Menhour, O. Sename, L. Dugard, B. D'Andréa-Novel, Integrated vehicle control through the coordination of longitudinal/lateral and vertical dynamics controllers: Flatness and LPV/h_∞-based design, International Journal of Robust and Nonlinear Control 27 (18) (2017) 4992–5007.

[43] S. Guo, S. Yang, C. Pan, Dynamic modeling of magnetorheological damper behaviors, Journal of Intelligent material systems and structures 17 (1) (2006) 3–14.

[44] M.-Q. Nguyen, O. Sename, L. Dugard, A motion-scheduled LPV control of full car vertical dynamics, in: Control Conference (ECC), 2015 European, IEEE, 2015, pp. 129–134.